Supplementary Figure 1

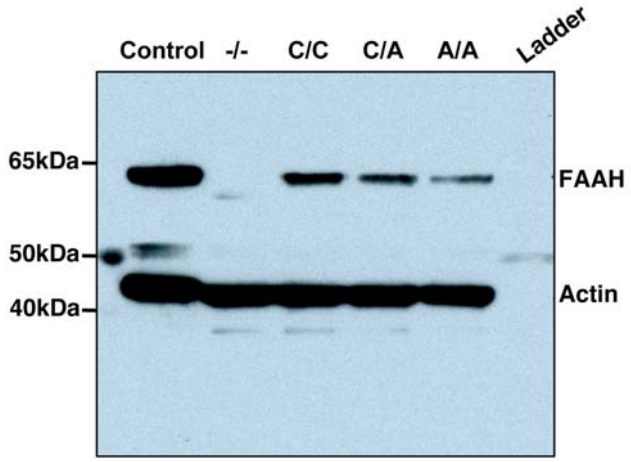

Supplementary Figure 1. Levels of FAAH protein in FAAH C385A mouse brain. A representative Western blot showing FAAH and actin protein levels in knock-in mice ($FAAH^{C/A}$; $FAAH^{A/A}$) and wild-type ($FAAH^{C/C}$) littermates from. Brain homogenates from $FAAH^{-/-}$ mice, and lysates from heterologous 293 cells overexpressing FAAH, were used as controls. The membrane was cut above the 50kDa molecular weight line and both FAAH and actin were immunoblotted simultaneously. The membrane was then realigned for exposure.

Supplementary Figure 2

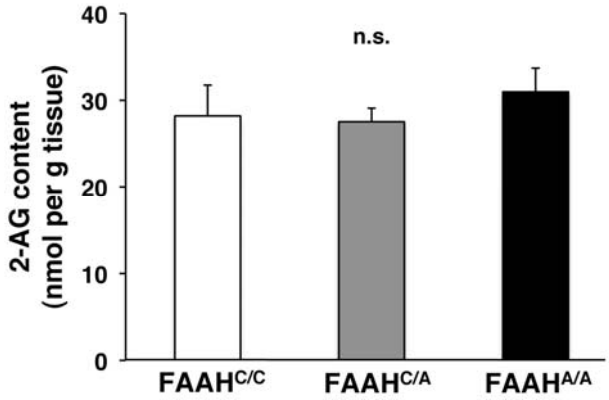

Supplementary Figure 2. Levels of the endocannabinoid 2-arachidonoylglycerol (2-AG) in FAAH C385A mouse brain. 2-AG content was assessed in FAAH knock-in mouse (n = 4) forebrain homogenates by mass spectrometry analysis. All results are presented as means ±SEM. (ANOVA with post-hoc Dunnett's test; [F(2,11)=0.44])

Supplementary Figure 3

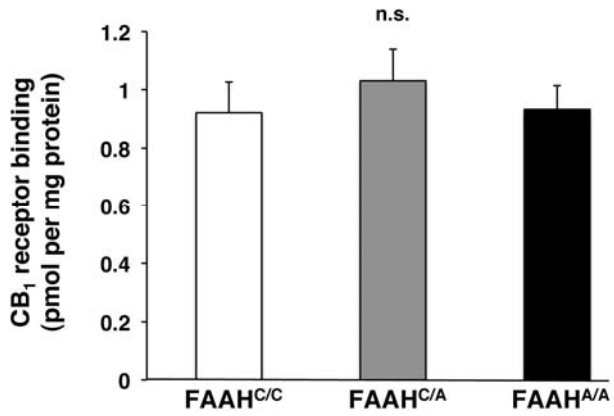

Supplementary Figure 3. CB_1 receptor binding site density in FAAH C365A mice. CB_1 receptor binding was assessed in FAAH knock-in mouse brain (n = 4) homogenates by radioligand binding assay. All results are presented as means ±SEM. (ANOVA with post-hoc Dunnett's test; [F(2, 11)=0.36])

Supplementary Figure 4

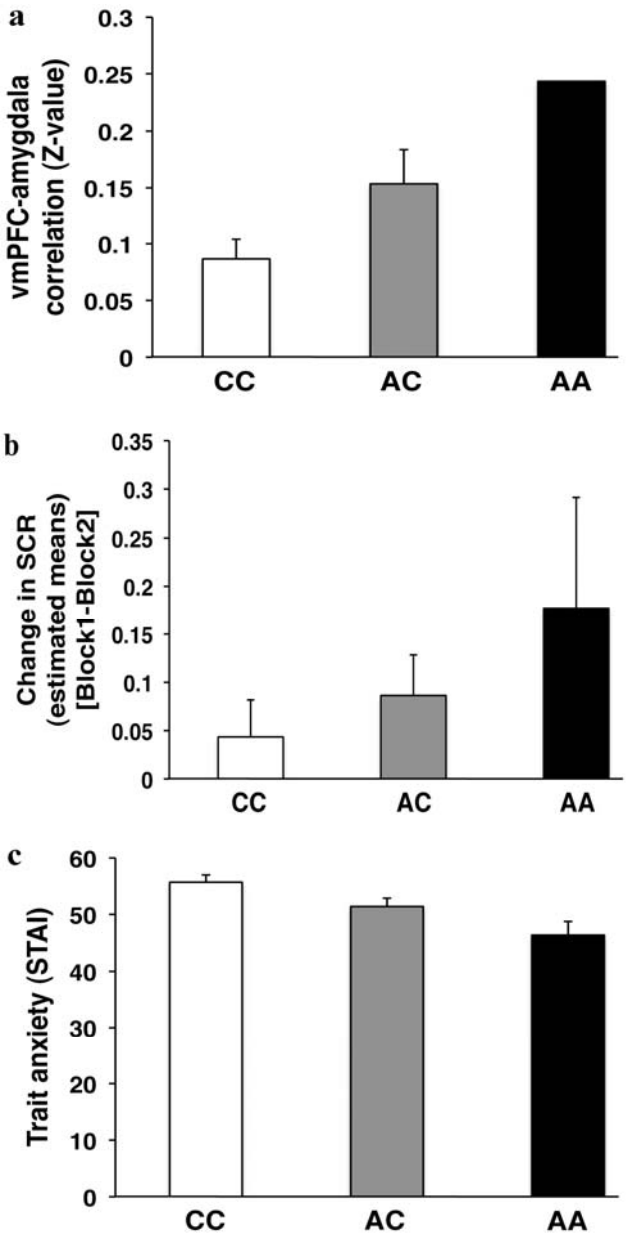

Supplementary Figure 4. Effect of FAAH C385A polymorphism in human cohorts plotted by three genotype groups. (**a**) Functional connectivity (AA: n = 1), (**b**) fear extinction (AA: n = 2), and (**c**) trait anxiety self-report (AA: n = 3) in human cohorts are plotted for each genotypic groups. Means ±SEM presented.

Supplementary Figure 5.

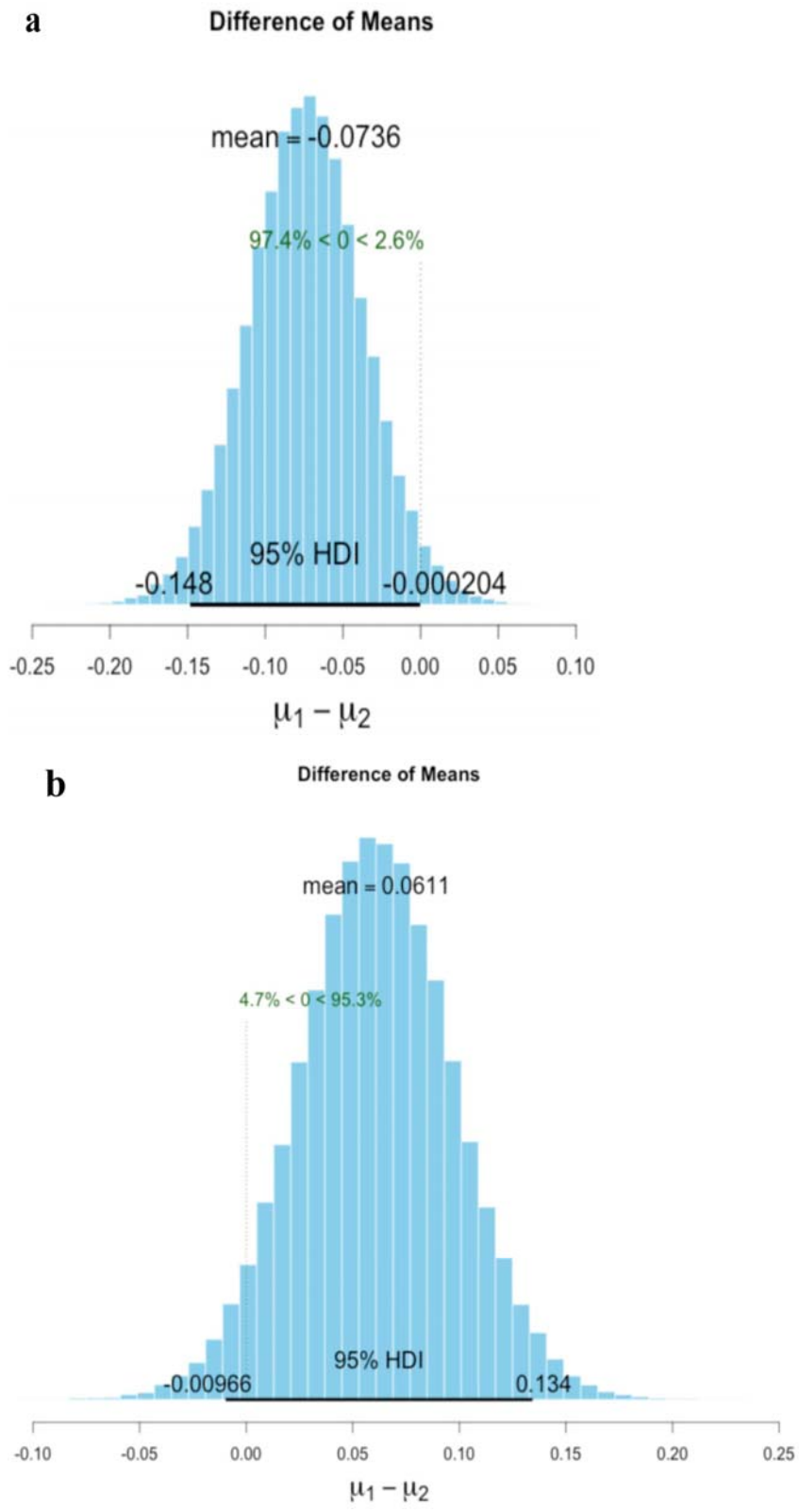

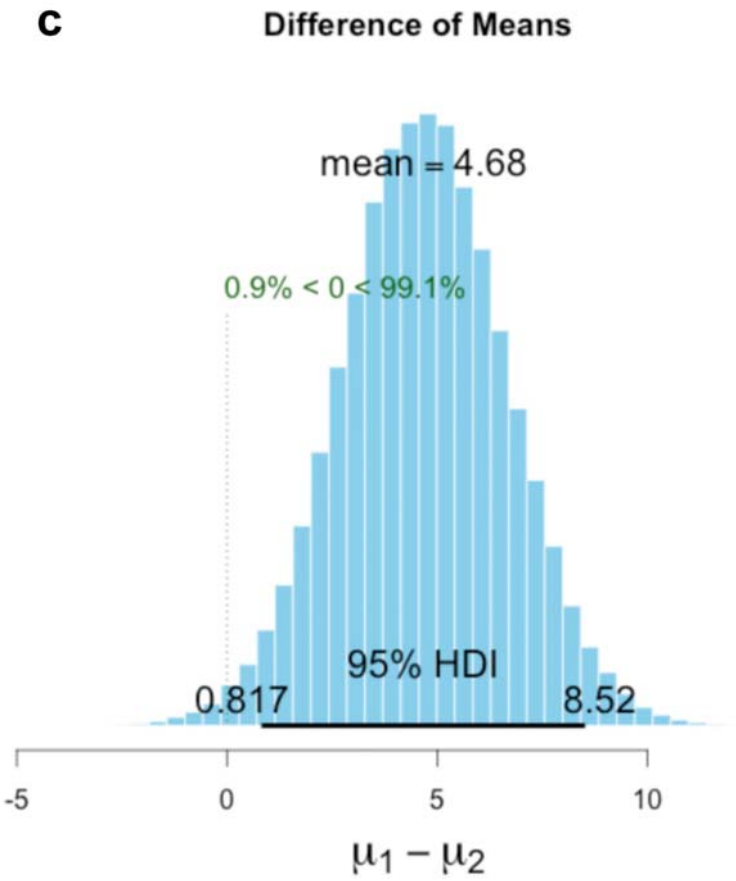

Supplementary Figure 5. Analysis of human findings using a Bayesian statistical approach. *FAAH* C385A polymorphism genotype group differences (A-allele carriers versus C homozygotes) in (**a**) resting state connectivity between vmPFC and amygdala ROIs (*P* = 0.026), (**b**) human fear extinction, late trial differential SCR (*P* = 0.047), and (**c**) trait anxiety self-report (*P* = 0.009) were re-analyzed using a Bayesian statistical approach without *a priori* assumptions of data distribution or variance.

Supplementary Figure 6

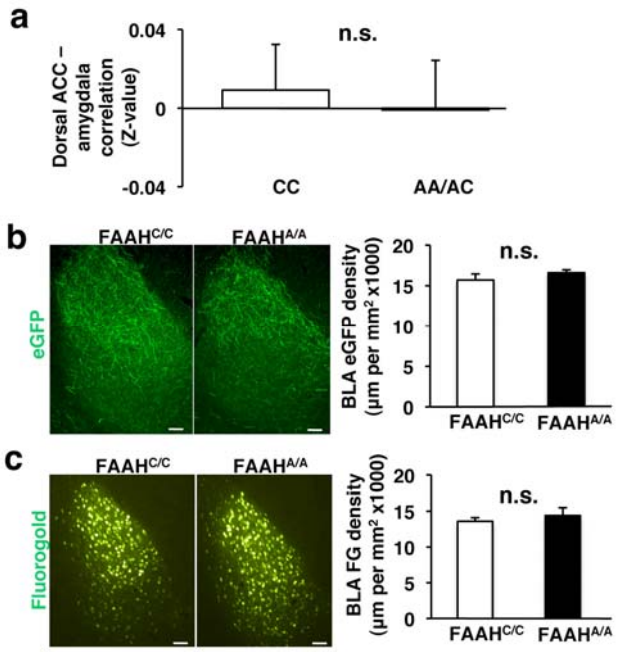

Supplementary Figure 6. vmPFC-amygdala connectivity in humans and mice with the *FAAH* C385A polymorphism. (**a**) BOLD fMRI functional connectivity comparing dorsal ACC and bilateral amygdala in A allele carriers (n = 17) relative to C homozygotes (n = 18) [t(33) = -0.28]. (**b**) Anterograde tracer (AAV2-eGFP; eGFP), targeted to PL, labeled afferents in the BLA in $FAAH^{A/A}$ mice (n = 4) and controls ($FAAH^{C/C}$, n = 4) (two-tailed Student's *t*-test). (**c**) Retrograde tracer (fluorogold; FG), targeted to PL, labeled BLA cell bodies in $FAAH^{A/A}$ mice (n = 4) and controls ($FAAH^{C/C}$, n = 4) (two-tailed Student's *t*-test). (Scale bars: 100µm) Means ±SEM presented.

Supplementary Figure 7

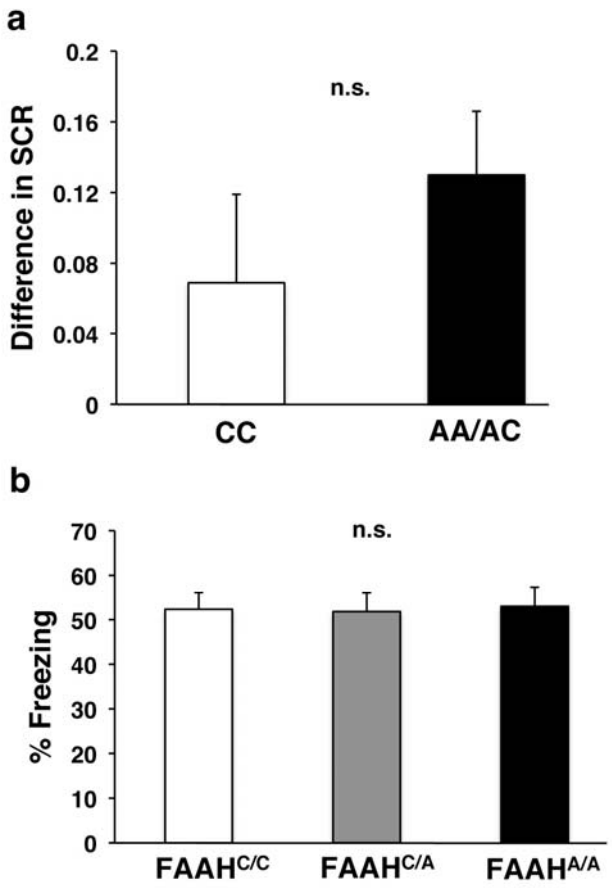

Supplementary Figure 7. Fear acquisition in humans and mice with the *FAAH* C385A polymorphism. (**a**) Fear acquisition in A-allele carriers (n = 18) relative to C homozygotes (n = 22) as measured by calculating differential skin conductance responses (SCR) between a cue previously paired with an aversive stimulus (CS+) and a cue never paired with an aversive stimulus (CS-) on the last 3 trials of acquisition [t(38) = -1.013]. (**b**) Fear acquisition in homozygous $FAAH^{A/A}$ (n = 21) and heterozygous $FAAH^{A/C}$ (n = 15) knock-in mice as well as littermate controls ($FAAH^{C/C}$, n = 11) was measured by freezing during the third acquisition tone. Means ±SEM presented. (ANOVA with post-hoc Dunnett's test; [F(2,44)=0.02])

Supplementary Figure 8

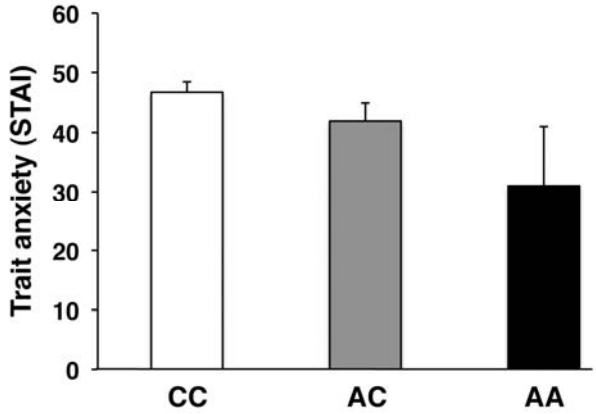

Supplementary Figure 8. Replication of inverse relationship between FAAH C385A and trait anxiety. Relationship between number of mutant *FAAH* C385A alleles and STAI trait anxiety was examined in the human fear extinction cohort revealing a significant negative correction (r(38)=-0.34, P = 0.031). This correlation is in the same direction as our initial self-report survey cohort (r(135) = -0.21, P = 0.014). Means ±SEM presented.

Supplementary Figure 9

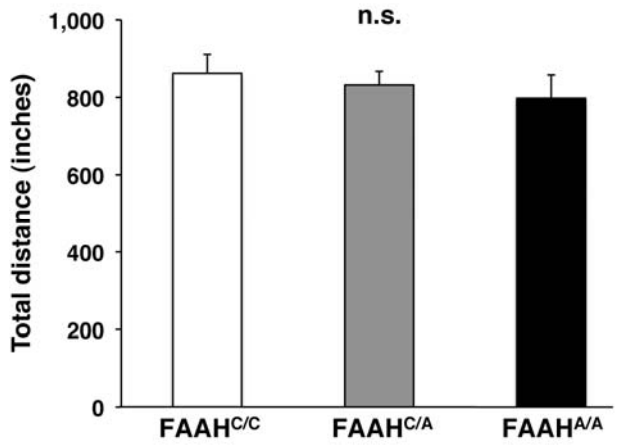

Supplementary Figure 9. Locomotor activity in FAAH C385A mice in the EPM test. Locomotor activity in the elevated plus maze was compared between wild type mice ($FAAH^{C/C}$, n = 17) and knock-in littermates ($FAAH^{C/A}$, n = 11; $FAAH^{A/A}$, n = 12) by measuring total distance traveled in a 10-minute session. All results are presented as means ±SEM. (ANOVA with post-hoc Dunnett's test; [F(2,37)=0.42])

Supplementary Table 1. Demographics of fMRI cohort

	C/C	A-allele carriers (A/A and A/C)	Total
	N = 18	N = 17	N = 35
Sex	10 Female; 8 Male	7 Female; 10 Male	17 Female; 18 Male
Mean Age (SD)	F: 20.80 (2.7) M: 19.75 (1.8)	F: 20.14 (2.2) M: 19.60 (1.90)	F: 20.53 (2.5) M: 19.67 (1.8)
Caucasian	(4F)	(5M)	26%
Asian	(2F, 1M)	(1F, 1M)	14%
African-American	(4F, 5M)	(4F, 1M)	40%
Hispanic	(2M)	(2F, 3M)	20%
Mixed	0	0	0%

Supplementary Table 2. Demographics of human fear extinction cohort

	C/C	A allele carriers (A/A and A/C)	Total
	N = 22	N = 18	N = 40
Sex	13 Female; 8 Male	8 Female; 10 Male	21 Female; 19 Male
Mean Age (SD)	F: 25.23 (2.8) M: 24.44 (4.7)	F: 20.25 (4.7) M: 23.00 (4.7)	F: 23.33 (4.3) M: 23.68 (4.6)
Caucasian	(5F, 3M)	(1F, 4M)	32.5%
Asian	(6F, 3M)	(1F, 3M)	32.5%
African-American	(2F, 3M)	(5F, 1M)	27.5%
Hispanic	0	(1F, 2M)	7.5%
Mixed	0	0	0%

Supplementary Table 3. Demographics of self-report survey cohort

	C/C	A allele carriers (A/A and A/C)	Total
	N = 80	N = 57	N = 137
Sex	49 Female; 31 Male	36 Female; 21 Male	85 Female; 52 Male
Mean Age (SD)	F: 20.65 (3.3) M: 21.03 (3.7)	F: 21.31 (3.4) M: 21.90 (4.4)	F: 20.93 (3.3) M: 21.38 (4.0)
Caucasian	(20F, 19M)	(12F, 12M)	46%
Asian	(22F, 11M)	(17F, 4M)	40%
African-American	0	(2F, 1M)	2%
Hispanic	(2F, 1M)	(3M)	4%
Mixed	(5F)	(5F, 1M)	8%